

# Mining geohazards susceptibility and risk mapping: The case of the Amyntaio open-pit coal mine, West Macedonia, Greece

P. Tzampoglou<sup>1</sup> · C. Loupasakis<sup>1</sup>

Received: 23 March 2017 / Accepted: 27 July 2017 / Published online: 8 August 2017  
© Springer-Verlag GmbH Germany 2017

**Abstract** During the last decades, numerous methodologies for the construction of both susceptibility and risk maps have been developed in order to identify and mitigate geohazards such as landslides and secondarily land subsidence phenomena caused by the collapse of natural or man-made underground cavities. According to literature review, the conducted research concerning the assessment of land subsidence risk due to the overexploitation of the aquifer is still at an early stage. This study focuses on the land subsidence phenomenon due to the overexploitation of the aquifer occurring in the Amyntaio basin in West Macedonia, hosting the active Amyntaio open-pit coal mine. This phenomenon has caused significant damage to settlements, farmlands and infrastructure. In order to construct susceptibility and risk maps knowledge of the geological, geotechnical, hydrogeological and tectonic settings of the study area is required. The proposed methodology for the production of a susceptibility and a risk map of land subsidence was based on the semi-quantitative method Weighted Linear Combination (WLC). The results were evaluated with an extensive field survey action recording, besides the above-mentioned settings, the spatial distribution of surface ruptures. The excellent agreement between the produced maps and the findings of the field survey, proved the added value of the maps, assigning them as crucial tools for the management of land subsidence phenomena.

**Keywords** Land subsidence · Susceptibility map · Risk map · GIS techniques · WLC method · Amyntaio basin

## Introduction

During the second half of the twentieth century, the over-exploitation of an aquifer triggered extensive land subsidence phenomena at numerous sites worldwide. The mechanism of this phenomenon has been studied by several researchers, aiming to estimate the connection between the deformation rates and the groundwater-level drop down (Burbey 2002; Galloway and Burbey 2011; Huang et al. 2012; Motagh et al. 2008; Pacheco-Martínez et al. 2013; Rothenburg et al. 1995; Wilson and Gorelick 1996; Xue et al. 2005). This anthropogenically induced natural hazard affects more than 150 big cities around the world (Hu et al. 2004). Some examples of this case are: Houston, USA (Buckley et al. 2003; Coplin et al. 1999), Arizona, USA (Conway 2016), Las Vegas Nevada, USA (Bell et al. 2002), New Jersey, USA (Sun et al. 1999), Shanghai, China (Chai et al. 2004), Hebei, China (Lv et al. 2014), Mexico City, Mexico (Chaussard et al. 2014; López-Quiroz et al. 2009; Ortiz-Zamora and Ortega-Guerrero 2010), Celaya, Mexico (Avila-Olivera et al. 2008), Morelia, Mexico (Cabral-Cano et al. 2010; Cigna et al. 2012), Tokyo, Japan (Ishii et al. 1970), Jakarta, Indonesia (Abidin et al. 2010, 2001), Semarang, Indonesia (Abidin et al. 2013; Lubis et al. 2011; Marfai and King 2007), Venice, Italy (Carbognin et al. 2004), Ravenna, Italy (Teatini et al. 2005) and Tehran, Iran (Dehghani et al. 2013; Mahmoudpour et al. 2016), etc.

In Greece, land subsidence, due to the over-pumping of aquifers, has been observed in several areas. In the wider Kalochori region, at the west of Thessaloniki, land

✉ P. Tzampoglou  
tzampogloup@gmail.com

<sup>1</sup> Laboratory of Engineering Geology and Hydrogeology, School of Mining and Metallurgical Engineering, National Technical University of Athens, 9 Heroon Polytechniou Str., 157 80 Zografou, Athens, Greece

subsidence was first noticed in 1964 in the form of Sea Water Intrusion (Loupasakis and Rozos 2009; Loupasakis et al. 1997; Psimoulis et al. 2007; Raspini et al. 2014; Rozos et al. 2000; Rozos et al. 2004; Svigkas et al. 2016). Currently, inland areas are located 4 m below sea level and embankments have been constructed to protect the village from flooding. In the Anthemounta plain, at the east end of Thessaloniki, increased pumping led, in 2005, to the occurrence of surface ruptures, causing damage to several buildings along the urban area of upper Peraia city. Recent studies evaluating persistent scatterer interferometry (PSI) data revealed that beside the narrow urban area of Peraia, the entire coastal zone of the plain has been affected by the phenomena (Raspini et al. 2016). In East Thessaly plain (Fakhri and Kalliola 2015; Ganas et al. 2006; Kontogianni et al. 2007; Salvi et al. 2004; Vassilopoulou et al. 2013), the systematic over-pumping of the aquifer for agricultural purposes has triggered land subsidence, initially observed in 1986. It is worth mentioning that according to data obtained by means of the PSI technique, seasonality of the land subsidence has been confirmed (Parcharidis et al. 2011). More specifically, the deformations rates during the dry season (August–September), when over-pumping of the aquifer for agricultural purposes is carried out, are much higher compared with the respectively deformations rates occurring during the wet season. Similar phenomena have been observed in the West Thessaly plain, with the first recorded land subsidence taking place in 1980 at the wider area of Farsala town (Rozos et al. 2010).

Various methodologies such as levelling networks, extensometers, GPS surveys and remote sensing (RS) have been applied for the study of the land subsidence phenomena. Each method has its own rules and restrictions. In the recent decades, especially in residential areas, interferometric synthetic aperture radar (INSAR) techniques, such as the persistent scatterer interferometry (PSI) technique, are widely used (Hsieh et al. 2011; Osmanoglu et al. 2011; Raspini et al. 2016; Yan et al. 2012). All these techniques can clearly identify the areas affected since the survey, but the land planning developers require some prognosis about their future extent. Such data can only be provided by designing land subsidence susceptibility and risk maps. According to the literature reviews, a methodology of risk assessment in land subsidence has been mainly applied to land subsidence phenomena triggered by the collapse of natural and man-made cavities as well as by the oxidation of organic soils (Choi et al. 2010; Galve et al. 2009; Kim et al. 2006; Ozdemir 2016; Park et al. 2012; Pradhan et al. 2014). Nothing relevant was found for areas affected by phenomena triggered by the overexploitation of aquifers. This is the main objective of the current work.

This research focuses on land subsidence due to the over-pumping of the aquifer conducted in order to protect

the slopes of an open-pit coal mine. The study area, Amyntaio basin, is located in West Macedonia at Florina prefecture (Fig. 1). It should be noted that this area includes numerous villages and that a part of the region is occupied by the Amyntaio open-pit coal mine.

During the last decades, the systematic over-pumping of the aquifer both by the mine activity and the agriculture works resulted in a significant groundwater-level drop. The drawdown of the aquifer along with the geotechnical and the tectonic characteristics of the area triggered land subsidence which caused significant damage to settlements and infrastructure. The mechanism of failure has been studied by many researchers (Loupasakis 2006, 2010; Loupasakis et al. 2014; Soulios et al. 2011; Tsourlos 2015; Tsourlos et al. 2007), but still some findings remain unclear. For example, the spatial distribution of the areas susceptible to land subsidence as well as the various mechanisms implicated at the manifestation of the phenomena (e.g. natural compaction and organic soils oxidation).

The main goal of the present study is to present a comprehensive methodology for the construction of both susceptibility and risk maps of land subsidence. To achieve this goal, all the factors which affect land subsidence (such as the tectonic, the geological and the hydrogeological ones) have been investigated and evaluated. The individually generated data were entered into an ARCGIS database; then, via spatial analysis, the respective maps have been constructed.

The land subsidence susceptibility and risk maps can be used by decision-making authorities for the assessment of the mining risk and the management and mitigation of the environmental impacts. Furthermore, they can be used by planners and engineers for future urban safety development reasons. Besides the importance of these maps to the local authorities, the applied methodology can be a guideline for further similar studies.

## Geological, geotechnical and hydrogeological setting of the study area

The Amyntaio basin is a part of the Pelagonian geotectonic zone of Greece and it is comprised of a crystalline-schist bedrock on which Neogene and Quaternary deposits have been deposited. The lithostratigraphic formulations of the study area can be divided into three main categories (Fig. 2):

### The Quaternary deposits

Their role has been of great importance in the manifestation of the land subsidence phenomena as the entire

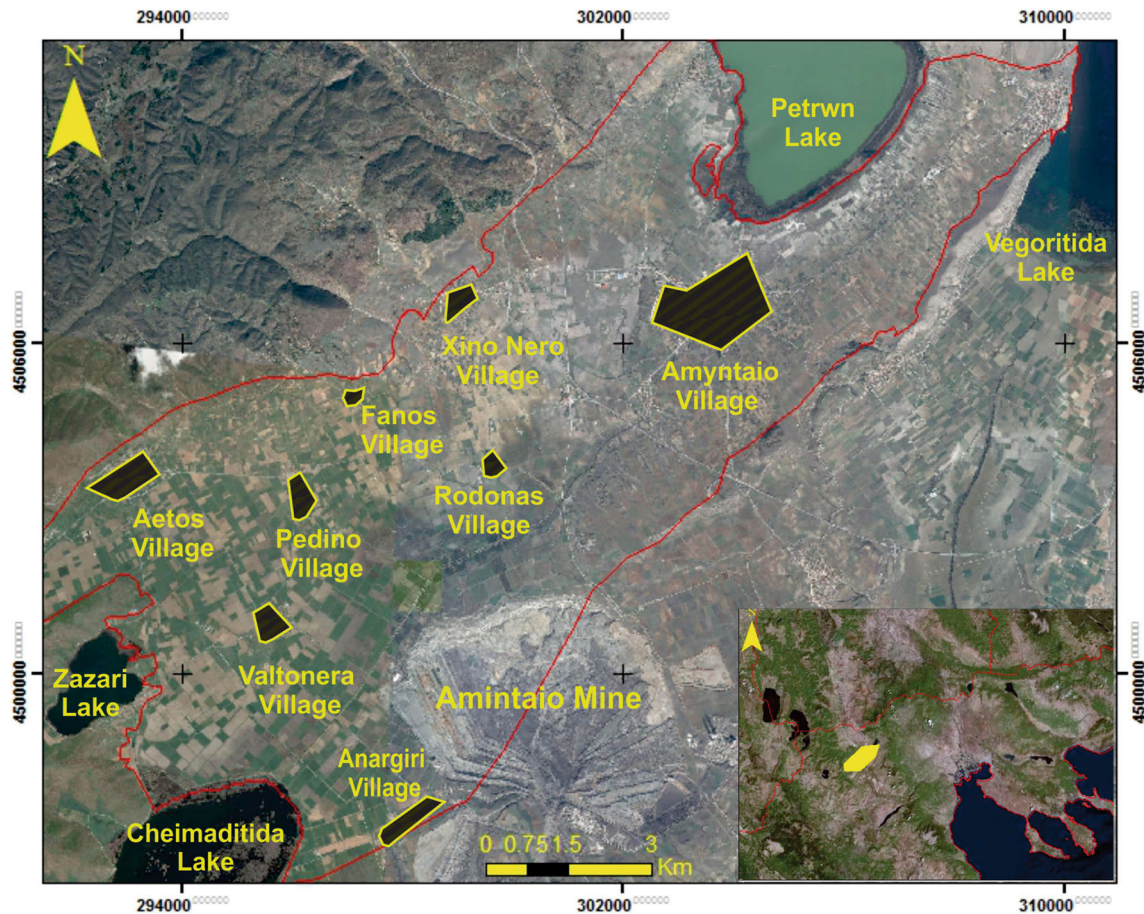


**Fig. 1** Study area delimited by the red outline

unconfined aquifer is developed exclusively within the Quaternary formation. So, these formations may be affected by the elevation drop of the aquifer. They are divided into:

**The Recent deposits:** They include the eluvial and the recent alluvial mantle, the clastic lacustrine deposits, and the old scree, talus cones. Furthermore, the Holocene travertines, the recent lacustrine, and the peat deposits are included in this category. These formations occupy most of the Amyntaio basin surface, even though they do not extend to great depth. According to the geotechnical data of these formations, it is clear that the lacustrine sandy silty clay as well as the peat deposits present high compression index values, with the average price reaching 0.187 and 1.707, respectively. They also contain large quantities of organics. Taking into account the fact that they both appear near to the surface, and therefore, they are not affected by a level drop of the aquifer, they can only be affected by oxidation.

**The Anargiroi Formation:** Middle-Pleistocene, fluvial-torrential sediments, consisting mainly of yellow-red silty-clayey sands with clay intercalations (I.G.M.E 1997). This formation presents low compression index with the average

price reaching the 0.083 for silty-clayey sand and the 0.133 for clay intercalations and high strength values. The fact that it is developed near to the surface and therefore is not affected by the drawdown of the aquifer in conjunction with their mechanical characteristics leads to the conclusion that it does not play an active role in the emergence of land subsidence phenomena.

**The Perdika's Formation:** Lower-Middle-Pleistocene river-lacustrine sediments, consisting of alternating layers of clayey sand, sandy clay, and sand with conglomerates (I.G.M.E 1997). In the upper stratum, they contain many organic materials forming organic silty-clay intercalation. According to the geotechnical data, this formation presents high compressibility index ( $C_c$ ) values with the average price reaching the 0.27 for the sandy silty clay and 0.99 for the organic silty clay. Thus, the Perdika's formation due to its structure and physicomechanical characteristics is susceptible to land subsidence in areas where water-level drawdown has been observed.

**The Proastio Formation:** Villafranchian age (I.G.M.E 1997) fluvial-torrential deposits, consisting mainly of alternating layers of silty-clayey sands and sandy gravels with red clays (Koukouzas et al. 1979). Sandy silty-clay

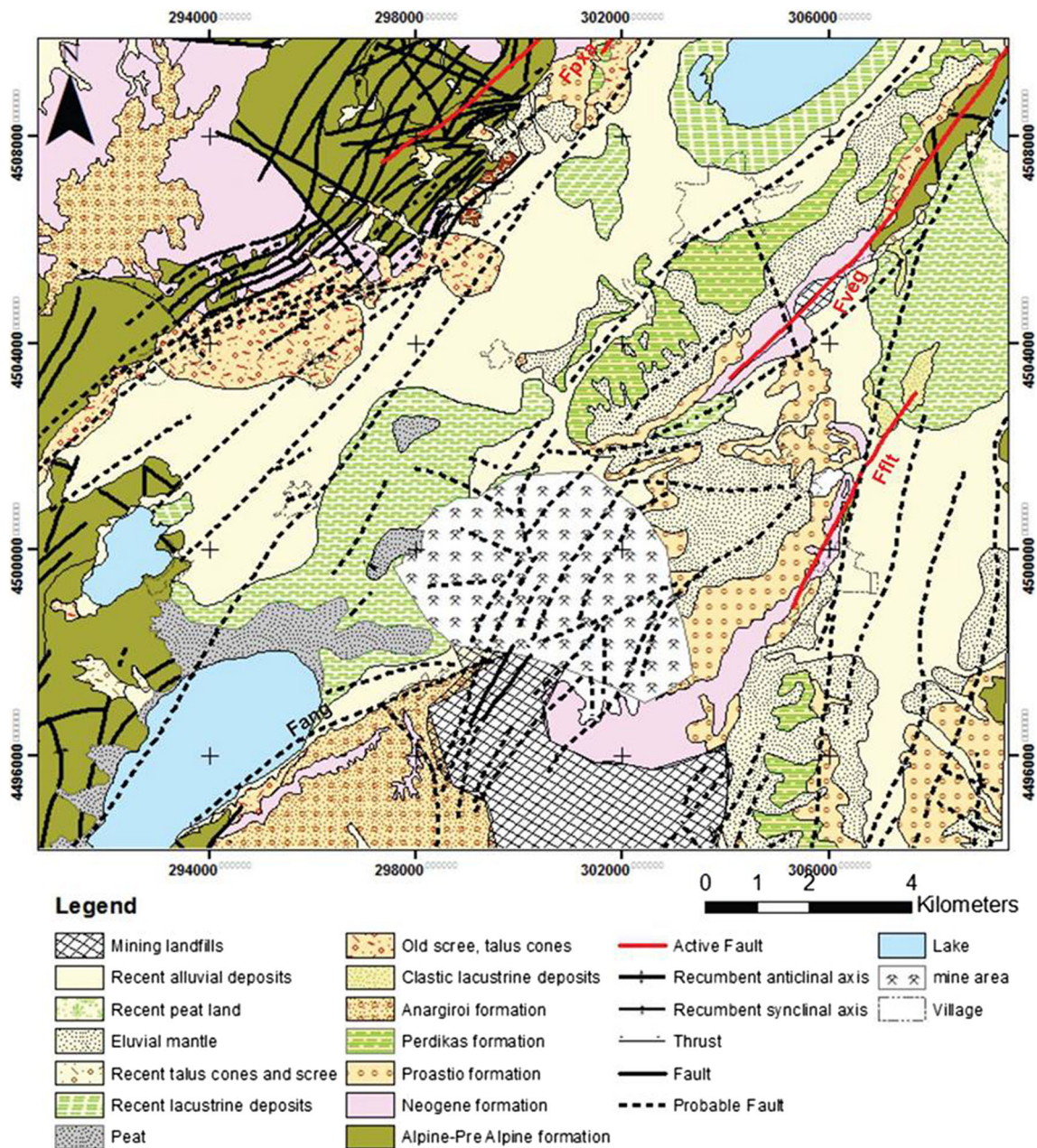


**Fig. 2** Geological map of the Amyntaio basin

horizons dominate at the deeper horizons. It presents a low compression index with the average value reaching the 0.16 for the sandy silty clay. Therefore, due to its mechanical characteristics, this formation is not susceptible to consolidation phenomena when the aquifer drawdown and effective stresses increase.

### Neogene formation

The Neogene formation can be distinguished in two series, the Lignite-bearing Ptolemaida Formation which is the

upper one and the Lignite-bearing Komnina Formation which is the lower one.

The Lignite-bearing Ptolemaida (upper series): Lacustrine-marshy deposits of the Pliocene age (I.G.M.E 1997), which consist mainly of alternating grey to grey-green silty clays and clayey sands (I.G.M.E 1997).

The Lignite-bearing Komnina Formation (lower series): Lacustrine-fluvial deposits of Upper Miocene–Lower Pliocene, which consist mainly of silty clays and sandy layers with intercalations of sandstones (I.G.M.E 1997).

Both formations are impermeable, and thus, they define the area affected by the overexploitation of the aquifer. Hence, due to their structure and their mechanical characteristics they preclude their rapid solidification even if the effective stresses increase.

### Alpine–pre-alpine formations

The Alpine and pre-Alpine formations are divided into the upper Palaeozoic metamorphic rocks, consisting of schists, crystalline schists gneiss, and quartzes and the Middle Triassic–Lower Jurassic carbonate cover consisting of marbles, crystalline limestones and tectonic breccias (Mountrakis 1985; Spyropoulos 1992).

The neotectonic activity of the wider study area is controlled by the ongoing Middle–Upper Miocene extensional strain field, which affects the northern part of the Greek territory (Mountrakis et al. 1998, 2006; Pavlides 1985; Pavlides and Simeakis 1988). According to the direction of the faults, identified in the Amyntaio basin, they can be distinguished into two groups: The older ones with NW–SE to NNW–SSE direction (Koukouzas et al. 1979; Koukouzas et al. 1983; Vetoulis 1951) affecting the Alpine–pre-Alpine formations (Pavlides 1985; Pavlides and Mountrakis 1985, 1987). The newer ones, with NE–SW to ENE–WSW direction, developed during the Pleistocene. The last ones formed the Ptolemaida–Amyntaio basin (Atzemoglou et al. 2003; Doutsos and Kokkalas 2001; Doutsos and Koukouvelas 1998; Koukouzas et al. 2000; Pavlides 1985). These faults intersect the Quaternary formations. Thus, they do play an active role in the occurrence of surface ruptures.

As presented in the geological map of Fig. 2, the study area is delimited by three main tectonic lines. The typical normal fault of Vegoritida (Fveg) with NNE–SSW direction along with the Anargiroi fault (Fang) borders the eastern end of the Amyntaio sub-basin. The Petron–Xino Nero–Aetos fault (Fpxa) with NE–SW direction borders the northwest side of the study area. It is important to notice that the Perdikas formation, which is susceptible to land subsidence, does not extend to the SE side of the Anargiroi fault (Koukouzas et al. 1981).

At this point, it should be noted that the faults presented on the geological map of Fig. 2 were verified by evaluating numerous studies (Ganas et al. 2015; I.G.M.E 1997; Pavlides 1985; Tsourlos 2015; Tsourlos et al. 2007) along with new field observation data.

The aquifer of Amyntaio basin is formed in the Quaternary deposits, reaching down to maximum depths of 120 m (Stamos and Giannouloupoulos 2010). The aquifer recharges by both karstic water inflow of the carbonate formations of the boundaries and by the filtration of surface water.

In 1989, the mining activities of the Amyntaio open-pit coal mine started and numerous wells, to protect the slopes

of the mine, were drilled. Although the majority of the over-pumped water was spouted to the surrounding irrigation canals, the aquifer was not recharged. This situation along with the overexploitation of the aquifer by the increasing number of farmers' irrigation wells changed radically the hydrogeological status of this area (Loupasakis et al. 2014).

The groundwater-level drop can be easily evaluated by designing the equal-drawdown contour lines between May 1992 and May 2015. The May 1992 piezometric data, referring to the hydrogeological conditions before the beginning of the mining activities, were provided by Dimitrakopoulos (2001). According to the distribution of the equal-drawdown contour lines (Fig. 3), an extensive depression cone was formed around the open pit. Furthermore, the isolated depression cones, away from the mine, indicate the contribution of the irrigation wells to the overexploitation of the aquifers (Tzampoglou and Loupasakis 2016).

### Methodology

In the research area, the causal factors affecting the land subsidence phenomena can be separated into two categories: the preparatory and the triggering causal factors. As preparatory causal factors, the geotechnical, the geological, and the tectonic settings of the study area can be considered. On the contrary, the only triggering factor has been the man-made overexploitation of the aquifers, both for the protection of the mine and for the irrigation of the farmlands. Due to the fact that land subsidence phenomena are driven by the consolidation mechanism and they are not affected by the stability of the open-pit slopes, the geometry of the excavation was not considered directly. Of course, the geometry of the excavation (perimeter) was indirectly introduced to the dataset by means of the isopiezometric lines as it diachronically affects their distribution around the mine (Fig. 3).

Taking into account the above factors, all necessary datasets have been collected. Besides the extensive literature review, several field campaigns were conducted aiming to collect data regarding the geological structure of the study area, to measure the seasonal groundwater-level variations, and to collect samples (56 in number) for the conduction of all necessary geotechnical laboratory tests. Generally, the data retrieved by the literature or obtained by the authors for the production of the susceptibility and the risk maps are:

1. The geological map of the study area. This map (Fig. 2) was produced by combining the field survey data with the geological map of the Institute of

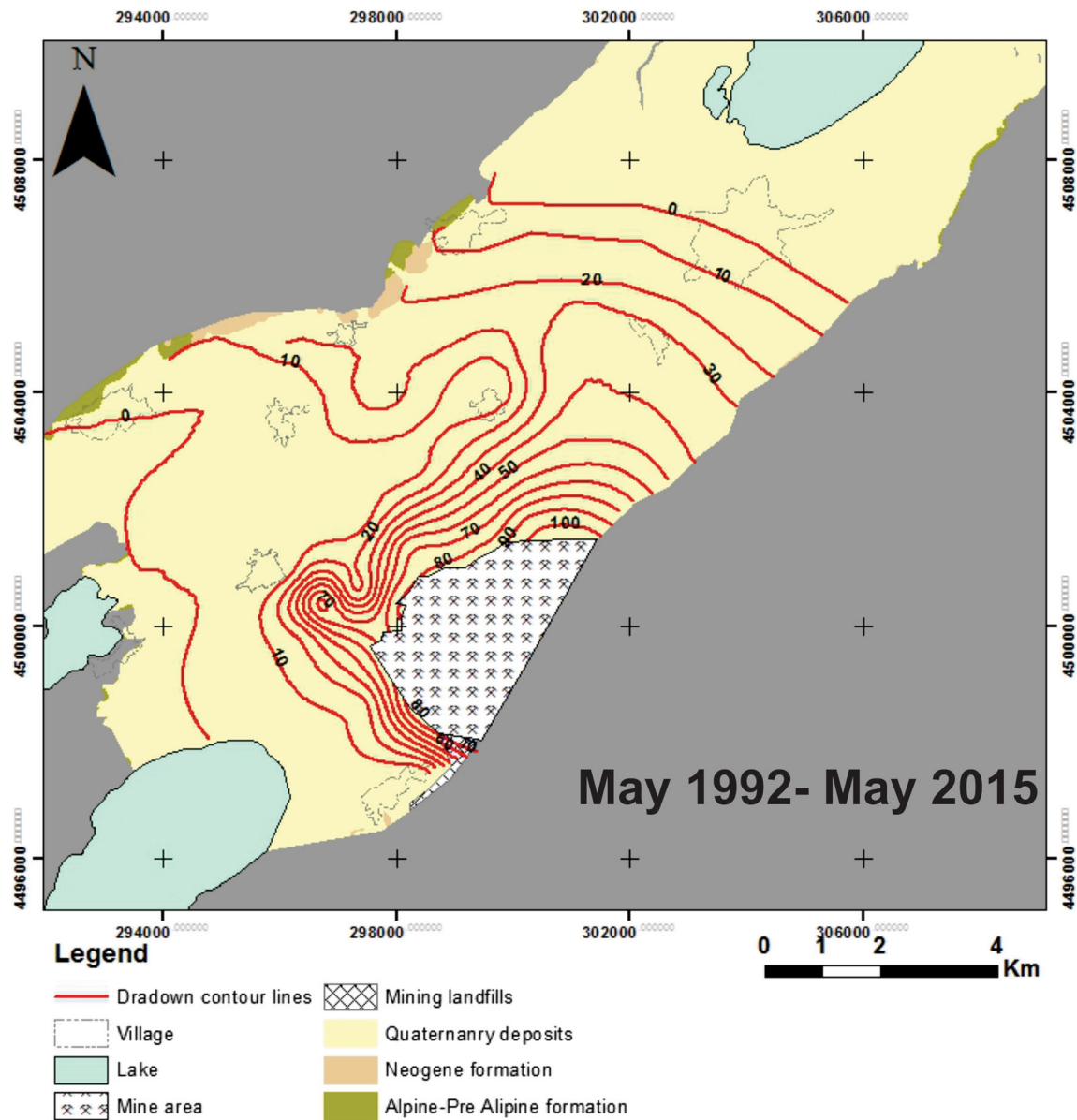


**Fig. 3** Equal-drawdown contour lines between May 1992 (Dimitrakopoulos 2001) and May 2015

- Geology and Mineral Exploitation (IGME) of Greece (I.G.M.E 1997).
- A detailed database with georeferenced geotechnical data, containing all the data derived from the literature review (Dimaras and Georgiadhs 2002; Doukissa 2010; Geoerevntiki 1980; Loupasakis 2010) and the laboratory tests conducted during the current study.
- The thematic geotechnical map of the Amyntaio basin, as produced by combining all above-mentioned geotechnical data with the geological maps and the field survey data.
- A detailed surface ruptures inventory map composed by combining data from all the field campaigns.
- The thematic hydrogeological maps presenting the isopiezometric contour lines at various dates, as produced by combining all available literature data (Dimitrakopoulos 2001; Loupasakis 2006, 2010; Loupasakis et al. 2014) with the field survey data. These data layers were further used for the production of equal-drawdown hydrogeological maps like the one presented in Fig. 3.
- The Corine Land Cover map of 2012 (Corine Land Cover 2012) for the land-use cover of the study area.

All above-described data have been introduced in the form of the thematic maps in ArcGIS. Afterwards, the land subsidence susceptibility and the risk maps were produced

by applying the Weighted Linear Combination (WLC) method (Ayalew and Yamagishi 2005).

**Layer preparation**

Based on the knowledge of the experts and in accordance with the requirement of the WLC method (Ayalew and Yamagishi 2005), all the above-described thematic layers were weighted and their classes were rated (Table 1). Then, the ArcGIS spatial analyst tool, providing useful applications for spatial modelling of risk assessment, has been used (Arnous et al. 2011). More specifically, GIS techniques including distance buffering, shapefile to raster conversion, reclassification, and raster calculations have been used. Finally, all the thematic maps have been digitized and converted to raster mode (10 × 10 m).

In order to produce the land subsidence susceptibility map, the following thematic layers have been used as follows:

*Geotechnical setting thematic layer*

Land subsidence due to the over-pumping of the aquifer is closely connected with the compressibility of the formations occupying the study area. Therefore, it was necessary to identify the compressibility index  $C_c$  of each soil formation. For that reason, 48 oedometer tests have been conducted, following ASTM standards, in order to enrich the mechanical parameters database composed by the literature data (Dimaras and Georgiadhs 2002; Doukissa 2010; Geoerevntiki 1980; Loupasakis 2010). It is worth emphasizing that these tests cannot be carried out in coarse grain layers. Of course, in geological formations consisting of alternating clayey, and sandy or coarse grain layers, the compressible clay layers determine the behaviour of the entire formation in regard to the land subsidence mechanism. The above-described database of geotechnical data had to be introduced as a thematic layer to the spatial modelling procedure. As all these data refer to particular points (the locations of the drills and the depth of the

**Table 1** Weights and class rates in land subsidence susceptibility based on ‘experts’ opinion

Thematic layers	Classes	Weight ( $W_j$ )	Rate ( $R_{ij}$ )
Geotechnical setting	Anthropogenic deposits	10	7
	Recent alluvial deposits		7
	Recent lacustrine deposits, peat land		10
	Eluvial mantle		7
	Recent talus cones and scree		5
	Peat		10
	Travertine		1
	Old scree, talus cones		5
	Clastic lacustrine deposits		10
	Anargiroi formation		6
	Perdikas formation		9
	Proastio formation		6
	Lignite-bearing Ptolemaida formation		1
	Lignite-bearing Komnina formation		1
	Tectonic structures–faults		Basin boundary faults (buffer)
400 m		10	
In-plain faults (buffer)			
200		9	
400		7	
600		5	
Groundwater-level drop	71–90	10	10
	51–70		9
	31–50		8
	11–30		7
	0–10		6
Thickness of ‘Perdikas’ formation	Higher thickness	8	10
	Medium thickness		8
	Lower thickness		6

samples), they had to be processed in order to obtain the mean values of the geotechnical parameters of each formation. So, the geotechnical data were statistically processed and the mean values of the geotechnical parameters were assigned according to the polygons representing the geological formations.

Finally, the formations were grouped together according to their mean compressibility index  $C_c$  values and the new simplified “geotechnical” map was rated (Table 1) and introduced to the model. The final geotechnical behaviour map is presented in Fig. 4a. The lacustrine and the peat deposits along with the Perdika’s formation are presented with the higher rates as, due to their high compression index values, are the main formations related to the land subsidence phenomena.

#### *Perdika’s formation thickness thematic layer*

As it was mentioned above, the Perdika’s formation, because of its mechanical properties, is susceptible to the manifestation of land subsidence in case of groundwater-level drop. The above-presented geotechnical setting thematic layer considers the surface coverage of the formation, but it cannot consider its thickness. Also, it does not consider its existence in areas that it is covered by alluvial deposits. So, the fact that this formation underlays the recent deposits and occupies a large part of the basin has to be introduced in a data layer. Also, it was necessary to construct a thematic layer with the variation of its thickness.

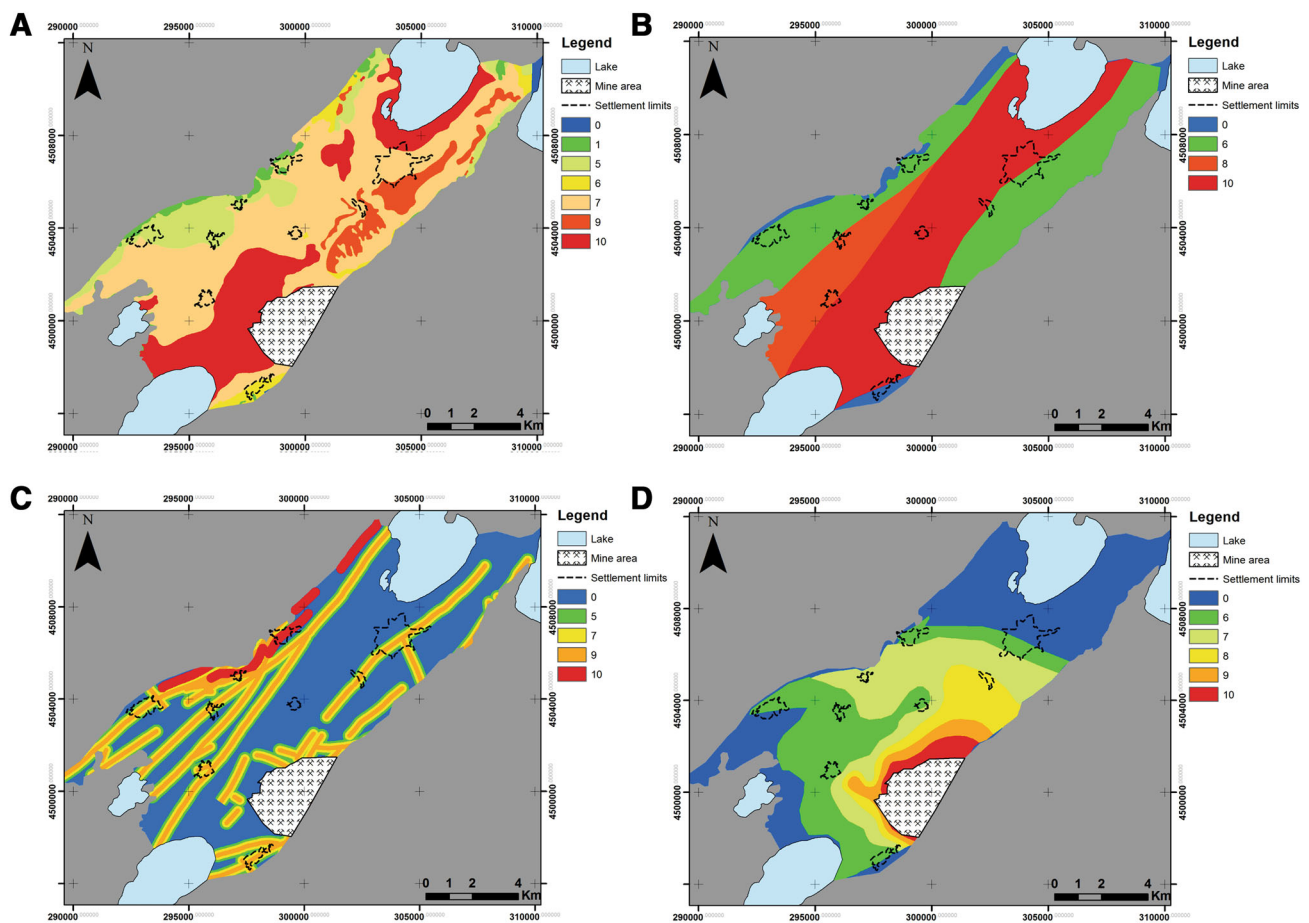


**Fig. 4** **a** The geotechnical setting thematic layer classifying the formations according to their compressibility index, from the lower (1) to the higher (10) values. **b** The Perdika's formation thickness thematic layer dividing the basin in segments with minimum (0) to maximum (10) thickness values. **c** The tectonic structure thematic layer indicating the areas presenting the maximum differential

deformation potential (values 10 and 9) due to their vicinity with the fault lines, and **d** the groundwater-level drop thematic layer dividing the plane to zones regarding the reduction in the piezometric surface from the maximum (10) to the minimum (1) values. The correlation between the rating values and the thematic layers' classes is clearly presented in Table 1



For that purpose, literature data including geophysical survey data and drill profiles of the study area were evaluated. Furthermore, data from the field survey along the slopes of the mine, reaching down to depths of 200 m, as well as tectonic data were also introduced to the data set. According this overall evaluation, a Perdika's formation thickness data layer was designed dividing the basin into four classes (Fig. 4b). The higher rates were assigned to the section covering the centre of the basin where the thickness of the formation reaches the maximum depth.

#### *Tectonic structure thematic layer*

The tectonic structure of the study area is of great importance in the occurrence of surface ruptures, which cause significant damage to buildings and infrastructure. This thematic layer is based on the geotectonic map included at the map of Fig. 2. For the purposes of this research, the faults were divided into two main categories: The in-plain faults and the basin boundary faults. The in-plain faults cross the plain intersecting formations with identical mechanical properties, and the boundary faults are located at the boundaries separating the Alpine–pre-Alpine formation and the Quaternary deposits.

The tectonic structure thematic layer introduced buffer zones around the faults, considering the width of the zone affected by the differential displacements along the faults and in accordance with the field survey data. So, at the basin boundary faults a buffer zone at a distance of 400 m was set. For the in-plain faults, multi-buffer zones at distances of 200, 400 and 600 m were set (Fig. 4c).

#### *Groundwater-level drop thematic layer*

The level drop of the aquifer is the main causal factor, which triggers the land subsidence in the Amyntaio basin. The specific thematic map was designed based on the equal-drawdown contour lines hydrogeological map between May 1992 and May 2015, as presented in Fig. 3. According to the values of the groundwater-level draw-down, this layer was distinguished in 6 classes (Fig. 4d).

### **Susceptibility map in land subsidence**

As above mentioned in order to design the susceptibility map, the semi-quantitative method of WLC was applied (Ayalew and Yamagishi 2005). According to this method for each raster cell of the map, a “Land Subsidence Susceptibility index (LSSI)” can result from the sum of the thematic layers rate multiplied by the appropriate weights (Kouli et al. 2010; Voogd 1983), according to the equation:

$$LSSI = \sum_{j=1}^n W_j * R_{ij} \quad (1)$$

$W_j$  The weight of each thematic layer,  $j$ ,  $R_{ij}$  The class rates  $i$  of each thematic layer  $j$ .

After the computing calculations, the susceptibility map of Fig. 5 was illustrated (). The results have been summarized following the geometrical interval method into five classes with very low, low, moderate, high and very high susceptibility. Evaluating the susceptibility map, some initial conclusions about the degree of influence of certain factors can be reached. First of all, a very high susceptibility in areas around the mine has been observed. This susceptibility decreases moving away from the open pit. This spatial distribution follows the thematic layer of the groundwater-level drop (Fig. 4d). Furthermore, in areas affected by faults, an increase in the total susceptibility index is evident. The effect on the thickness of the formation caused by the offset of the faults is the main reason of this phenomenon. It is worth noting that the areas within the limits of the basin, near the basin boundary faults, have been marked as high susceptibility ones. This is due to the difference in stiffness between the pre-Alpine rock or the Neogene soft rock formations and the Quaternary sediments which allow the manifestation of surface ruptures, even when low differential displacements occurred.

### **Validation of susceptibility maps**

In order to validate the susceptibility map, the detailed surface ruptures inventory map (Fig. 6) was used. The numerous field campaigns indicated that the surface ruptures mainly spread between the Anargiroi and Valtonera settlements. The surface ruptures direction is parallel to the tectonic lines developed during Pleistocene with a NE–SW direction. The larger differential deformations occur in the sections of the surface ruptures located near the open pit, with offset values reaching up to 0.5–1.0 m. The settlements mainly affected by the surface ruptures are Anargiroi, Valtonera, and Fanos, where extensive damages to buildings and infrastructure have been recorded.

The land subsidence susceptibility map is clearly verified by the inventory map, recording 15.545 m of surface ruptures (Fig. 6). As presented in Fig. 7, illustrating both the susceptibility and the inventory maps, all the recorded surface ruptures are located into the very high to high LSSI areas. Particularly, 75% of the ruptures were found in areas characterized with very high and 25% in areas characterized with high susceptibility index. Moreover, the settlements affected by the phenomena are also included inside the very high to high susceptibility areas.

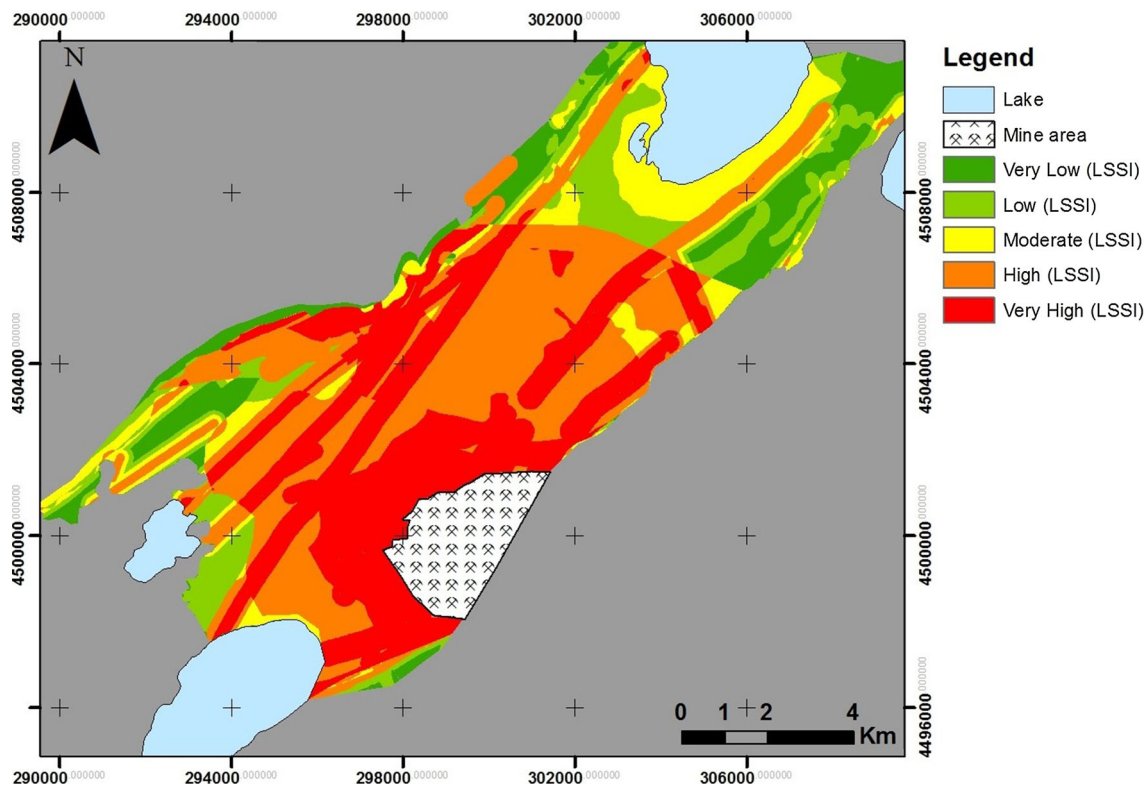


**Fig. 5** Land Subsidence Susceptibility Index (LSSI) map at the Amyntaio basin

### Land subsidence risk map

Land subsidence phenomena caused by the overexploitation of the aquifers are “quiet” catastrophic events, as they can be taking place for several years without being noticed, especially at the beginning. Due to the relatively slow deformation rates, they cannot be considered directly as life-threatening events. On the other hand, they can cause extremely severe financial damage as they can affect settlements, infrastructure, networks, and farm lands in areas extending hundreds of square kilometres. To this extent, human life can be threatened when damages to infrastructure or buildings lead gradually to failures.

In order to produce the land subsidence risk map, two new thematic layers considering the elements at risk were introduced to the model. These thematic layers refer to the land use and the road network (Fig. 8). The class rating and weighting of the exposure factors were based on the consequences caused by the land subsidence phenomena mainly on economic loss (Table 2). Generally, the higher rates were given by the experts in residential areas and in regions with particular economic interest in order to determine the impact of the land subsidence. The elements in land subsidence risk (LSR) are calculated by the equation:

$$\text{LSR} = \text{LSSI} * \text{Exposure} \quad (2)$$

where

$$\text{Exposure} = \sum_{j=1}^n W'_j * R'_{ij} \quad (3)$$

$W'_j$ : The weight of each thematic layer,  $j$ , referring to the element at risk  
 $R'_{ij}$ : The class rates  $i$  of each thematic layer  $j$  referring to the element at risk.

Evaluating the produced risk map (Fig. 9), it appears that all the settlements around the open pit and over major tectonic lines could be affected by land subsidence as they are located in a high- or very-high-risk area. Therefore, the urban planning in these areas should be done very carefully. Furthermore, a great part of the Amyntaio plain, which is characterized as high- or very-high-risk area, is mainly used for agricultural purposes. This reflects the economic consequences caused by the destruction of drills, farmhouses, and generally infrastructure. Regarding the road network, the financial impact is significant as, due to the differential deformations, continuing improvement works are required.

### Discussion and conclusion

In the Amyntaio basin, the areas susceptible to the manifestation of land subsidence should meet certain conditions. These include the presence of formations with high compressibility index rates (such as the Perdikas formation)

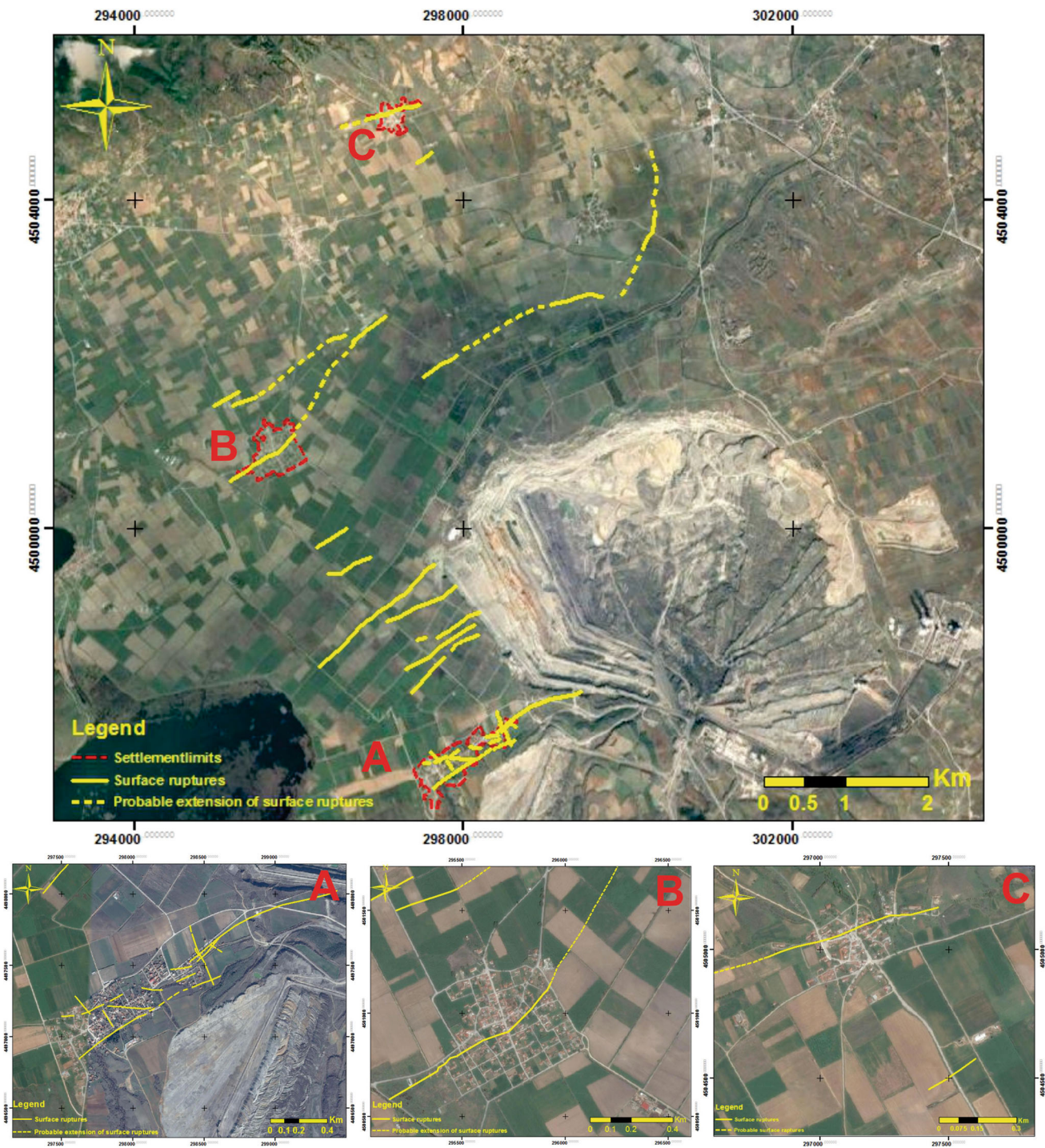


**Fig. 6** Distribution of the surface ruptures at the Amyntaio basin. **a** Surface ruptures recorded at the Anargiroi village, **b** at the Valtонера village and, **c** at the Fanos village

and the intensive groundwater-level drop. Furthermore, in places where tectonic structures intersect the sediments, causing intensive offset of the compressible sediments' thicknesses, the differential displacements can trigger extensive surface ruptures.

The produced susceptibility map, which takes into account all the preparatory and triggering causal factors, seems to be in high correlation with the field observation. Particularly, at the villages of Anargiroi, Fanos, and Valtонера where the three above-mentioned conditions do

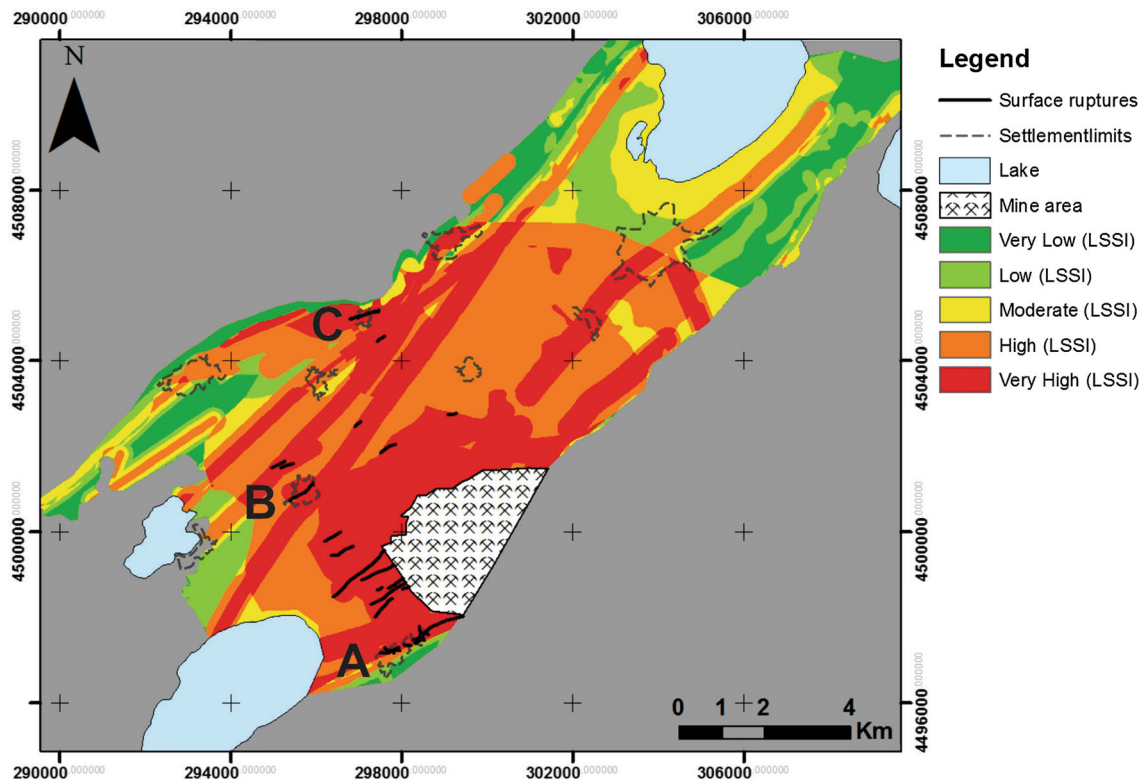


**Fig. 7** Susceptibility map in land subsidence along with the recorded surfaces ruptures. **a** Anargiroi village. **b** Valtonera village and. **c** Fanos village

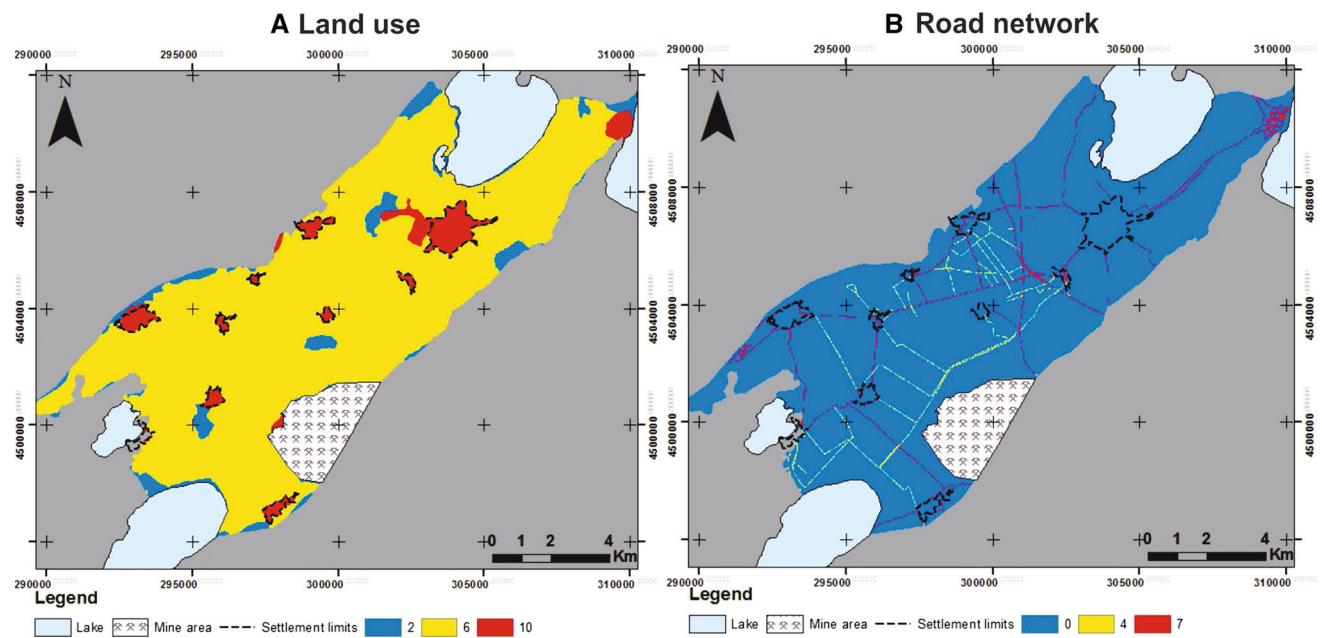


**Fig. 8** **a** Land-use thematic layer rated according to the impact of the land subsidence. The residential areas were rated with the higher score (10). **b** The road network thematic layer, the primary network

was rated with higher scores than the secondary network. The correlation between the rating values and the data layers' classes is clearly presented in Table 2

occur, the susceptibility map fits perfectly with the inventory map recording the surface ruptures (Fig. 6). For instance, in the settlement of Anargiroi the groundwater

drawdown decreases when moving away from the mine (towards the SW) resulting in the reduction in the surface ruptures. This observation fits perfectly with the

**Table 2** Weights and class rates referring to the elements at risk based on experts' opinion

Data layers	Classes	Weight ( $W'_j$ )	Rate ( $R'_{ij}$ )
Land use	Urban areas, industrial zones, archaeological sites	10	10
	Croplands, vineyards and land with fruit trees		6
	Grasslands, forests, mining areas, lakes		2
Road network	Primary road network	6	7
	Secondary road network		4

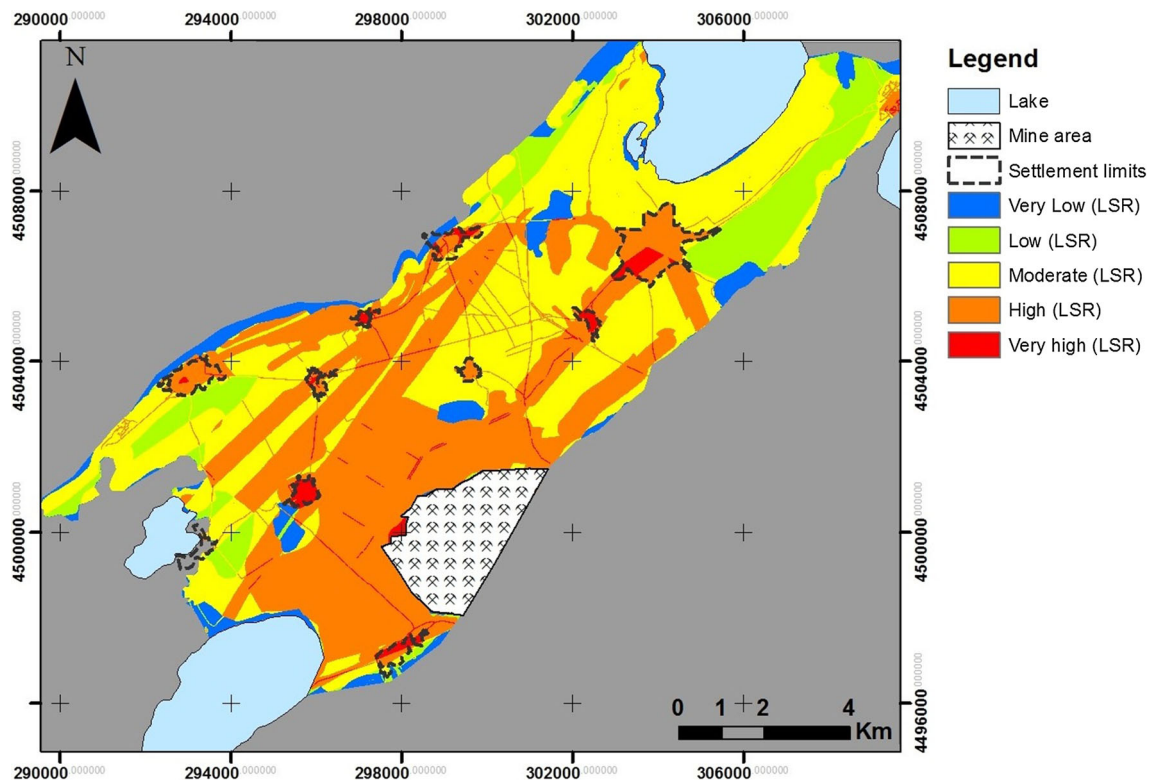


**Fig. 9** Land subsidence risk (LSR) map at the Amyntaio basin

susceptibility map in which the classification decreases from very high to high and finally to moderate with respect to the distance from the open pit.

In other settlements where no surface ruptures have been recorded, it is not precluded that land subsidence has occurred. There is a strong possibility that land subsidence occurs, but due to the absence of tectonic structures, no differential displacements and as a result no surface ruptures occur. For this reason, some further investigation using surface levelling or remote sensing techniques should be conducted in the settlements of Pedino and Sotiras, where both the Perdikas formation and the depression cone of the aquifer extend. Furthermore, some additional investigation should be conducted at the Xino Nero settlement which, according to the produced map, is highly susceptible to land subsidence. This settlement is founded along the geological boundary of the scree materials with the Quaternary deposits and is intersected by the active

fault of Petron-Xino Nero-Aetos (fpxa), but due to the small groundwater-level drop differential displacements have not yet been recorded. Concerning Aetos settlement, despite the fact that it is developed over the Perdika's formation and is affected by the basin boundary fault, it is out of the depression cone, and therefore, differential displacements, as expected, were not recorded. This is also in agreement with the susceptibility map.

So, it is clear that the verification by the field data has confirmed the accuracy of the very-high- and high-risk areas and generally the overall accuracy of the susceptibility map. Respectively, the land subsidence risk map supported by the susceptibility map provides accurate information about the areas exposed to risks, supporting their mitigation.

In conclusion, the proposed methodology for the construction of the land subsidence susceptibility and risk maps was proved to be accurate. The WLC method,

although depending on the knowledge of experts, in cases where the quality of the available data is high and the expert provides the right class rating and weighting of the thematic layer, the results can be rewarding.

## References

- Abidin HZ, Djaja R, Darmawan D, Hadi S, Akbar A, Rajiyowiryono H, Sudibyo Y, Meilano I, Kasuma M, Kahar J (2001) Land subsidence of Jakarta (Indonesia) and its geodetic monitoring system. *Nat Hazards* 23:365–387
- Abidin HZ, Andreas H, Gamal M, Gumilar I, Napitupulu M, Fukuda Y, Deguchi T, Maruyama Y, Riawan E (2010) Land subsidence characteristics of the Jakarta Basin (Indonesia) and its relation with groundwater extraction and sea level rise Groundwater response to changing climate. *IAH Sel Pap hydrogeol* 16:113–130
- Abidin H, Andreas H, Gumilar I, Sidiq TP, Fukuda Y (2013) Land subsidence in coastal city of Semarang (Indonesia): characteristics, impacts and causes *Geomatics. Nat Hazards Risk* 4:226–240
- Amous MO, Aboulela HA, Green DR (2011) Geo-environmental hazards assessment of the north western Gulf of Suez Egypt. *J Coast Conserv* 15:37–50
- Atzemoglou A, Tsourlos P, Pavlides S (2003) Investigation of the tectonic structure of the NW part of the Amynteon basin (NW Greece) by means of a vertical electrical sounding (VES) survey. *J Balk Geophys Soc* 6:188–201
- Avila-Olivera JA, Farina P, Garduño-Monroy VH, Oleschko K, Cherkasov S, Prieto JLP, Argüelles VT, Salado CIG, Miranda AGC, Castro SAZ (2008) Integration of InSAR and GIS in the study of surface faults caused by subsidence-creep-fault processes in Celaya, Guanajuato Mexico. *AIP Conf Proc* 1:200–211
- Ayalew L, Yamagishi H (2005) The application of GIS-based logistic regression for landslide susceptibility mapping in the Kakuda-Yahiko Mountains. *Cent Jpn Geomorphol* 65:15–31
- Bell JW, Amelung F, Ramelli AR, Blewitt G (2002) Land subsidence in Las Vegas, Nevada, 1935–2000: new geodetic data show evolution, revised spatial patterns, and reduced rates. *Environ Eng Geosci* 8:155–174
- Buckley SM, Rosen PA, Hensley S, Tapley BD (2003) Land subsidence in Houston, Texas, measured by radar interferometry and constrained by extensometers. *J geophys Res Solid Earth* 108(B11). doi:10.1029/2002JB001848
- Burbey TJ (2002) The influence of faults in basin-fill deposits on land subsidence, Las Vegas Valley, Nevada, USA. *Hydrogeol J* 10:525–538
- Cabral-Cano E, Arciniega-Ceballos A, Díaz-Molina O, Cigna F, Osmanoglu B, Dixon T, DeMets C, Vergara-Huerta F, Garduño-Monroy V, Ávila-Olivera J (2010) Is there a tectonic component on the subsidence process in Morelia, Mexico? In: Land subsidence, associated hazards and the role of natural resources development. *Hydrological Sciences Journal, Red Book Series*, vol 339. IAHS Publication, pp 164–169
- Carbognin L, Teatini P, Tosi L (2004) Eustacy and land subsidence in the Venice Lagoon at the beginning of the new millennium. *J Mar Syst* 51:345–353
- Chai J, Shen S, Zhu H, Zhang X (2004) Land subsidence due to groundwater drawdown in Shanghai. *Geotechnique* 54:143–147
- Chaussard E, Wdowinski S, Cabral-Cano E, Amelung F (2014) Land subsidence in central Mexico detected by ALOS InSAR time-series. *Remote Sens Environ* 140:94–106
- Choi J-K, Kim K-D, Lee S, Won J-S (2010) Application of a fuzzy operator to susceptibility estimations of coal mine subsidence in Taebaek City, Korea. *Environ Earth Sci* 59:1009–1022
- Cigna F, Osmanoglu B, Cabral-Cano E, Dixon TH, Ávila-Olivera JA, Garduño-Monroy VH, DeMets C, Wdowinski S (2012) Monitoring land subsidence and its induced geological hazard with synthetic aperture radar interferometry: a case study in Morelia, Mexico. *Remote Sens Environ* 117:146–161
- Conway BD (2016) Land subsidence and earth fissures in south-central and southern Arizona, USA. *Hydrogeol J* 24:649–655
- Coplin LS, Galloway D, Ingebritsen E (1999) Land subsidence in the United States. *US Geol Surv Circ* 1182:35–48
- Corine Land Cover 2012 (2012) <http://land.copernicus.eu/pan-european/corine-land-cover/clc-2012/view>, Accessed on 20 Mar 2015
- Dehghani M, Zoj MJV, Hooper A, Hanssen RF, Entezam I, Saatchi S (2013) Hybrid conventional and Persistent Scatterer SAR interferometry for land subsidence monitoring in the Tehran Basin, Iran. *ISPRS J photogramm Remote Sens* 79:157–170
- Dimaras k, Georgiadhs M (2002) Lifting and waterproofing Study of the existing embankment of Lake Cheimaditida Florina. Geognosi A.E. Unpublished report, Thessaloniki
- Dimitrakopoulos D (2001) Hydrogeological conditioning of Amynteon mine. Problems during exploitation and overcoming them. PhD Dissertation, National Technical University of Athens, Athens
- Doukissa K (2010) Geotechnical study of the bridge in the central trench of Aanargiroi area, municipality of Aetos. Unpublished report, Thessaloniki
- Doutsos T, Kokkalas S (2001) Stress and deformation patterns in the Aegean region. *J Struct Geol* 23:455–472
- Doutsos T, Koukouvelas I (1998) Fractal analysis of normal faults in northwestern Aegean area, Greece. *J Geodyn* 26:197–216
- Fakhri F, Kallioli R (2015) Monitoring ground deformation in the settlement of Larissa in Central Greece by implementing SAR interferometry. *Nat Hazards* 78:1429–1445
- Galloway DL, Burbey TJ (2011) Review: regional land subsidence accompanying groundwater extraction. *Hydrogeol J* 19:1459–1486
- Galve J, Gutiérrez F, Lucha P, Guerrero J, Bonachea J, Remondo J, Cendrero A (2009) Probabilistic sinkhole modelling for hazard assessment. *Earth Surf Proc Landf* 34:437–452
- Ganas A, Salvi S, Atzori S, Tolomei C (2006) Ground deformation in Thessaly, Central Greece, retrieved from Differential Interferometric analysis of ERS-SAR data. In: Abstract Volume of the 11th International Symposium on Natural and Human Induced Hazards & 2nd Workshop on Earthquake Prediction, Patras, Greece
- Ganas A, Oikonomou I, Tsimi A (2015) NOA faults: a digital database for active faults in Greece. *Bull Geol Soc Greece* 47:518–530
- Geoerevnikiti E (1980) AHS Amyntaiou, Preliminary geotechnical investigation. Public Power Corporation S.A. Unpublished report, Athens
- Hsieh C-S, Shih T-Y, Hu J-C, Tung H, Huang M-H, Angelier J (2011) Using differential SAR interferometry to map land subsidence: a case study in the Pingtung Plain of SW Taiwan. *Nat Hazards* 58:1311–1332
- Hu R, Yue Z, Wang Lu, Wang S (2004) Review on current status and challenging issues of land subsidence in China. *Eng Geol* 76:65–77
- Huang B, Shu L, Yang Y (2012) Groundwater overexploitation causing land subsidence: hazard risk assessment using field observation and spatial modelling. *Water Res Manag* 26:4225–4239
- I.G.M.E. (1997) Geological map of Greece, scale 1:50,000, Ptolemaida sheet. I.G.M.E., Athens

- Ishii M, Kuramochi F, Endo T (1970) Recent tendencies of the land subsidence in Tokyo. *Proc Int Assoc Hydrol Symp* 121:25–34
- Kim K-D, Lee S, Oh H-J, Choi J-K, Won J-S (2006) Assessment of ground subsidence hazard near an abandoned underground coal mine using GIS. *Environ Geol* 50:1183–1191
- Kontogianni V, Pytharouli S, Stiros S (2007) Ground subsidence, Quaternary faults and vulnerability of utilities and transportation networks in Thessaly, Greece. *Environ Geol* 52:1085–1095
- Koukoulas C, Kotis T, Ploumidis M, Metaxas A (1979) Coal exploration of Anargiri-Amynteon area. Mineral deposit research vol No 9. I.G.M.E, Athens
- Koukoulas C, Kotis T, Ploumidis M, Metaxas A (1981) Coal exploration of “Apophisis” field of Anargiri–Amynteon area. Research for energy resources vol No1. I.G.M.E, Athens
- Koukoulas C, Kotis T, Ploumidis M, Metaxas A, Dimitriou D (1983) Coal exploration of Komninon-Ptolemaidas area. Mineral deposit research vol No2. I.G.M.E, Athens
- Koukoulas C, Kotis T, Metaxas A, Ploumidis M, Varvarousis I, Dimitriou D, Ioakim C (2000) Potential of lignite deposits and palaeoclimatic evolution of Ptolemais basin during the Neogene–Quaternary period *Proc Interim Colloquium RCMNS* (Patras, Greece, May 1998). *Geol Soc Greece Spec Pub* 9:151–162
- Kouli M, Loupasakis C, Soupios P, Vallianatos F (2010) Landslide hazard zonation in high risk areas of Rethymno Prefecture, Crete Island, Greece. *Nat Hazards* 52:599–621
- López-Quiroz P, Doin M-P, Tupin F, Briole P, Nicolas J-M (2009) Time series analysis of Mexico City subsidence constrained by radar interferometry. *J Appl Geophys* 69:1–15
- Loupasakis C (2006) Study of the geotechnical conditions of the Amintaio coalmine slopes close to the Anargiri village, Aetos Municipality, Florina Prefecture, Greece, Unpublished report I.G.M.E, Athens
- Loupasakis C (2010) Geotechnical works in the Anargiroi village, Aetos Municipality, Florina Prefecture, Greece. Unpublished report I.G.M.E., Athens
- Loupasakis C, Rozos D (2009) Finite-element simulation of land subsidence induced by water pumping in Kalochori village, Greece. *Q J Eng Geol Hydrogeol* 42:369–382
- Loupasakis C, Sotiriadis M, Soulios G (1997) Hydrochemical characteristics of the underground water of the plain area located between Thessaloniki and N. Halkidona. In: *Proceedings of the 4th Hydrogeological Congress of the Hellenic Hydrogeological Committee and the Association of Geologists and Mineralogists of Cyprus, Thessaloniki, Hellenic Committee of Hydrogeology, Thessaloniki*, pp 194–212
- Loupasakis C, Angelitsa V, Rozos D, Spanou N (2014) Mining geohazards—land subsidence caused by the dewatering of opencast coal mines: the case study of the Amyntaio coal mine, Florina, Greece. *Nat Hazards* 70:675–691
- Lubis AM, Sato T, Tomiyama N, Isezaki N, Yamanokuchi T (2011) Ground subsidence in Semarang-Indonesia investigated by ALOS–PALSAR satellite SAR interferometry. *J Asian Earth Sci* 40:1079–1088
- Lv F, Ma X, Zhao C, Song W (2014) The distribution and causes of ground fissures on the Hebei Plain. *Shanghai Land Res (Chin)* 35:49–53
- Mahmoudpour M, Khamehchiyan M, Nikudel MR, Ghassemi MR (2016) Numerical simulation and prediction of regional land subsidence caused by groundwater exploitation in the southwest plain of Tehran, Iran. *Eng Geol* 201:6–28
- Marfai MA, King L (2007) Monitoring land subsidence in Semarang Indonesia. *Environ Geol* 53:651–659
- Motagh M, Walter TR, Sharifi MA, Fielding E, Schenk A, Anderssohn J, Zschau J (2008) Land subsidence in Iran caused by widespread water reservoir overexploitation. *Geophys Res Lett.* doi:10.1029/2008GL038314
- Mountrakis D (1985) *Geology of Greece*. University studio Press, Thessaloniki
- Mountrakis D, Pavlides S, Zouros N, Astaras T, Chatzipetros A (1998) Seismic fault geometry and kinematics of the 13 May 1995 Western Macedonia (Greece) earthquake. *J Geodyn* 26:175–196
- Mountrakis D, Tranos M, Papazachos C, Thomaidou E, Karagianni E, Vamvakaris D (2006) Neotectonic and seismological data concerning major active faults, and the stress regimes of Northern Greece. *Geol Soc Lond Spec Publ* 260:649–670
- Ortiz-Zamora D, Ortega-Guerrero A (2010) Evolution of long-term land subsidence near Mexico City: review, field investigations, and predictive simulations. *Water Res Res.* doi:10.1029/2008WR007398
- Osmanoğlu B, Dixon TH, Wdowinski S, Cabral-Cano E, Jiang Y (2011) Mexico City subsidence observed with persistent scatterer InSAR. *Int J Appl Earth Obs Geoinf* 13:1–12
- Ozdemir A (2016) Sinkhole susceptibility mapping using logistic regression in Karapınar (Konya, Turkey). *Bull Eng Geol Env* 75:681–707
- Pacheco-Martínez J, Hernández-Marín M, Burbey TJ, González-Cervantes N, Ortiz-Lozano JÁ, Zermeño-De-Leon ME, Solís-Pinto A (2013) Land subsidence and ground failure associated to groundwater exploitation in the Aguascalientes Valley, Mexico. *Eng Geol* 164:172–186
- Parcharidis I, Fomelis M, Katsafados P (2011) Seasonal ground deformation monitoring over Southern Larissa Plain (Central Greece) by SAR interferometry. In: *Advances in the Research of Aquatic Environment*, Springer, Berlin, pp 497–504
- Park I, Choi J, Lee MJ, Lee S (2012) Application of an adaptive neuro-fuzzy inference system to ground subsidence hazard mapping. *Comput Geosci* 48:228–238
- Pavlides S (1985) Neotectonic evolution of the Florina-Vegoritiss-Ptolemais basin (W. Macedonia, Greece). PhD Dissertation, Aristotle University of Thessaloniki
- Pavlides S, Mountrakis D (1985) Neotectonics of the Florina-Vegoritiss-Ptolemais Neogene Basin (NW Greece): an example of extensional tectonics of the greater Aegean area. In: *Annales géologiques des pays helléniques*, vol 1. Laboratoire de géologie de l’Université, pp 311–327
- Pavlides S, Mountrakis D (1987) Extensional tectonics of northwestern Macedonia Greece, since the late Miocene. *J Struct Geol* 9:385–392
- Pavlides S, Simeakis K (1988) Neotectonics and active tectonics in low seismicity areas of Greece: vegoritiss (NW Macedonia) and Melos is 1 Complex-Comparison. *Ann Geol des Pays Hellen* 33:176–191
- Pradhan B, Abokharima MH, Jebur MN, Tehrany MS (2014) Land subsidence susceptibility mapping at Kinta Valley (Malaysia) using the evidential belief function model in GIS. *Nat Hazards* 73:1019–1042
- Psimoulis P, Ghilardi M, Fouache E, Stiros S (2007) Subsidence and evolution of the Thessaloniki plain, Greece, based on historical leveling and GPS data. *Eng Geol* 90:55–70
- Raspini F, Loupasakis C, Rozos D, Adam N, Moretti S (2014) Ground subsidence phenomena in the Delta municipality region (Northern Greece): geotechnical modeling and validation with Persistent Scatterer Interferometry. *Int J Appl Earth Obs Geoinf* 28:78–89
- Raspini F, Bianchini S, Moretti S, Loupasakis C, Rozos D, Duro J, Garcia M (2016) Advanced interpretation of interferometric SAR data to detect, monitor and model ground subsidence: outcomes from the ESA-GMES TerraFirma project. *Nat Hazards* 83:155–181
- Rothenburg L, Obah A, El Baruni S (1995) Horizontal ground movements due to water abstraction and formation of earth

- fissures. In: Proceedings of the Fifth International Symposium on Land Subsidence. International Association of Hydrological Sciences 234:239–249
- Rozos D, Apostolidis E, Christaras B (2000) Engineering–geological map of Thessaloniki wider area. In: Proceedings of National Meeting on Protection of Thessaloniki from Natural Hazards, Thessaloniki, pp 46–53
- Rozos D, Apostolidis E, Xatzinakos I (2004) Engineering-geological map of the wider Thessaloniki area Greece. *Bull Eng Geol Environ* 63:103–108
- Rozos D, Sideri D, Loupasakis C, Apostolidis E (2010) Land subsidence due to excessive ground water withdrawal. A case study from Stavros-Farsala site, West Thessaly, Greece. In: 12th International Congress of the Geological Society of Greece. *Bull Geol Soc Greece* 43(4):1850–1857
- Salvi S, Ganas A, Stramondo S, Atzori S, Tolomei C, Pepe A, Manzo M, Casu F, Berardino P, Lanari R (2004) Monitoring long-term ground deformation by SAR Interferometry: examples from the Abruzzi, Central Italy, and Thessaly, Greece. In: 5th International Symposium on Eastern Mediterranean Geology. Thessaloniki, Greece, pp T7–T17
- Soulios G, Tsapanos T, Voudouris K, Kaklis T, Mattas C, Sotiriadis M (2011) Ruptures on surface and buildings due to land subsidence in Anargyri village (Florina Prefecture, Macedonia). *Advances in the Research of Aquatic Environment*. Springer, Berlin, pp 505–512
- Spyropoulos N (1992) The geological structure of Pelagonian zone in the Mount of Askio D. Macedonia. PhD Dissertation, Aristotle University of Thessaloniki
- Stamos A, Giannouloupoulos P (2010) Hydrogeological report, Geotechnical work to the Anargiri village, Aetos Municipality, Florina Prefecture, Greece. Unpublished report I.G.M.E., Athens
- Sun H, Grandstaff D, Shagam R (1999) Land subsidence due to groundwater withdrawal: potential damage of subsidence and sea level rise in southern New Jersey, USA. *Environ Geol* 37:290–296
- Svigkas N, Papoutsis I, Loupasakis C, Tsangaratos P, Kiratzi A, Kontoes C (2016) Land subsidence rebound detected via multi-temporal InSAR and ground truth data in Kalochori and Sindos regions, Northern Greece. *Eng Geol* 209:175–186
- Teatini P, Ferronato M, Gambolati G, Bertoni W, Gonella M (2005) A century of land subsidence in Ravenna, Italy. *Environ Geol* 47:831–846
- Tsourlos P (2015) Research for the appearance of surface cracks in the Valtonea village, Amyntaio Municipality, Florina Region. School of Geology of the Aristotle University of Thessaloniki Aristotelian University of Thessaloniki, Thessaloniki
- Tsourlos P, Papazaxos C, Bargmeziw G, Koutalou B (2007) Investigation and suggestions for the problem created by the fault which as appeared in municipalities of Fanos and Ksino Nero. School of Geology of the Aristotelian University of Thessaloniki, Thessaloniki
- Tzampoglou P, Loupasakis K (2016) New data regarding the ground water level changes at the Amyntaio basin-Florina Prefecture, Greece. In: Proceedings of the 14th International Congress of the Geological Society of Greece, Thessaloniki, Bulletin of the Geological Society of Greece, vol. No 2, pp 1006–1015
- Vassilopoulou S, Sakkas V, Wegmuller U, Capes R (2013) Long term and seasonal ground deformation monitoring of Larissa Plain (Central Greece) by persistent scattering interferometry. *Cent Eur J Geosci* 5:61–76. doi:10.2478/s13533-012-0115-x
- Vetoulis D (1951) Lignite basin of Amyntaio-Vegora vol 14. Geological IGEF recognition
- Voogd H (1983) Multi-Criteria Evaluations for Urban and Regional Planning. Princeton University, London
- Wilson AM, Gorelick S (1996) The effects of pulsed pumping on land subsidence in the Santa Clara Valley. *Calif J hydrol* 174:375–396
- Xue Y-Q, Zhang Y, Ye S-J, Wu J-C, Li Q-F (2005) Land subsidence in China. *Environ Geol* 48:713–720
- Yan Y, Doin M-P, Lopez-Quiroz P, Tupin F, Fruneau B, Pinel V, Trouvé E (2012) Mexico city subsidence measured by InSAR time series: joint analysis using PS and SBAS approaches. *IEEE J Sel Top Appl Earth Obs Remote Sens* 5:1312–1326